Electrochemistry

DOI: 10.1002/ange.201410569

Photoelectrochemical Hydrogen Production in Alkaline Solutions Using Cu_2O Coated with Earth-Abundant Hydrogen Evolution Catalysts**

*Carlos G. Morales-Guio, Laurent Liardet, Matthew T. Mayer, S. David Tilley, Michael Grätzel, and Xile Hu**

Abstract: *The splitting of water into hydrogen and oxygen molecules using sunlight is an attractive method for solar energy storage. Until now, photoelectrochemical hydrogen evolution is mostly studied in acidic solutions, in which the hydrogen evolution is more facile than in alkaline solutions. Herein, we report photoelectrochemical hydrogen production in alkaline solutions, which are more favorable than acidic solutions for the complementary oxygen evolution half-reaction. We show for the first time that amorphous molybdenum sulfide is a highly active hydrogen evolution catalyst in basic medium. The amorphous molybdenum sulfide catalyst and a Ni–Mo catalyst are then deposited on surface-protected cuprous oxide photocathodes to catalyze sunlight-driven hydrogen production in 1M KOH. The photocathodes give photocurrents of $-6.3\,mA\,cm^{-2}$ at the reversible hydrogen evolution potential, the highest yet reported for a metal oxide photocathode using an earth-abundant hydrogen evolution reaction catalyst.*

The splitting of water using sunlight energy in a photoelectrochemical (PEC) cell is a promising method to produce renewable hydrogen.[1,2] The water splitting process consists of two half-reactions: the hydrogen evolution reaction (HER; $2H^+ + 2e^- \rightarrow H_2$) at the cathode and the oxygen evolution reaction (OER; $2H_2O \rightarrow O_2 + 4H^+ + 4e^-$) at the anode. Because ionic conductivity is highest at extreme pH values, and the electric current in the electrolyte should be carried only by protons or hydroxide ions, photoelectrochemical water splitting is commonly carried out in either highly acidic or highly alkaline solutions. Whereas the hydrogen evolution is more facile when the concentration of protons is high, oxygen evolution is easier when the concentration of hydroxide is high.[3] As the overpotential loss for the OER tends to be several-fold higher than for the HER when state-of-the-art electrocatalysts are applied, the efficiency of PEC water splitting should be higher in basic medium than in acidic medium. Furthermore, in basic solutions a number of abundant and inexpensive metal oxide catalysts exhibit comparable and even higher OER activity than rare and expensive RuO_x and IrO_x catalysts, whereas in acidic solutions only RuO_x and IrO_x are good catalysts.[4–6] With more desirable OER catalysts available for use in alkaline solutions, we were therefore motivated to develop photocathodes capable of efficiently evolving hydrogen in basic medium. These photocathodes might then be combined with either a solar cell or a photoanode to obtain a tandem device for unassisted water splitting in alkaline solutions. Significant progress has been made in PEC hydrogen evolution in acidic and even neutral solutions,[7–11] however, to the best of our knowledge, only $CaFe_2O_3$ has been reported as a photocathode for PEC hydrogen evolution in alkaline solutions.[12] However, the efficiency of solar energy conversion was very low as the incident photon to current conversion efficiency (IPCE) in the visible-light region was below 5%. Herein, we show that amorphous molybdenum sulfide and Ni–Mo catalysts can be coupled to surface-protected Cu_2O photocathodes to produce hydrogen in alkaline solutions with efficiency comparable to analogous devices in acidic solutions.

We have recently shown that electrochemically deposited amorphous molybdenum sulfide films are an active hydrogen evolution catalyst.[13,14] The catalyst is more active in acidic solutions than in neutral and slightly basic solutions.[13] We reported that different electrochemical deposition methods gave precatalysts that are composed of different proportions of amorphous MoS_3 and MoS_2, yet during hydrogen evolution, all precatalysts were converted into the same active species MoS_{2+x}.[15] While examining the activity of the catalyst in alkaline solutions, we noticed that different precatalysts had drastically different stability in 1M KOH. If the precatalyst contains MoS_3, then it is quickly dissolved in the electrolyte. If the precatalyst contains no MoS_3, then it is

---

[*] C. G. Morales-Guio, L. Liardet, Prof. Dr. X. L. Hu
Laboratory of Inorganic Synthesis and Catalysis
Institute of Chemical Sciences and Engineering
École Polytechnique Fédérale de Lausanne (EPFL)
ISIC-LSCI, BCH 3305, 1015 Lausanne (Switzerland)
E-mail: xile.hu@epfl.ch
Homepage: http://lsci.epfl.ch

Dr. M. T. Mayer, Dr. S. D. Tilley, Prof. Dr. M. Grätzel
Laboratory of Photonics and Interfaces
Institute of Chemical Sciences and Engineering
École Polytechnique Fédérale de Lausanne (EPFL)
1015 Lausanne (Switzerland)

[**] This work is supported by a starting grant from the European Research Council (ERC), number 257096 to X.L. Hu, the Swiss Federal Office for Energy (PECHouse Competence Center, contract number SI/500090-02), the PECDEMO project (co-funded by Europe's Fuel Cell and Hydrogen Joint Undertaking under Grant Agreement No. 621252), the PHOCS project (European Union, ENERGY 2012-10.2.1, Future Emerging Technologies Collaborative Project no. 309223), and the European Research Council under the Advanced Research Grant (ARG 247404) "Mesolight" to M.G.

Supporting information for this article is available on the WWW under http://dx.doi.org/10.1002/anie.201410569.

stable in 1 M KOH. Figure S1 and Supporting Movie 1 show the results of treating two precatalysts on fluorine-doped tin oxide (FTO) with one drop of 1 M KOH. The MoS_3–AE film was deposited by constant anodic electrolysis (AE) and contains mainly amorphous MoS_3. Upon contact with the KOH solution, this film quickly delaminated from the FTO and was dissolved in a few seconds. The MoS_{2+x}–CE film was deposited by constant cathodic electrolysis (CE) and contains already the active MoS_{2+x} catalyst but not MoS_3. This film is stable in 1 M KOH solution.

Figure 1 a shows the HER activity of the MoS_{2+x}–CE catalyst (loading: 20 μg cm^{-2}) on FTO in 1 M KOH. The overpotential for a current density of 10 mA cm^{-2} is about 310 mV. In comparison, the same electrode reaches 10 mA cm^{-2} at $\eta = 235$ mV in 1 M H_2SO_4. Figure S2 (see the Supporting Information, SI) shows that the HER activity of MoS_{2+x}–CE is stable during 10 h. Although amorphous molybdenum sulfides and MoS_2 nanoparticles are by now well-established HER catalysts in acidic solutions,[14,16–19] this is the first time they are shown as active and stable HER catalysts in basic solutions.

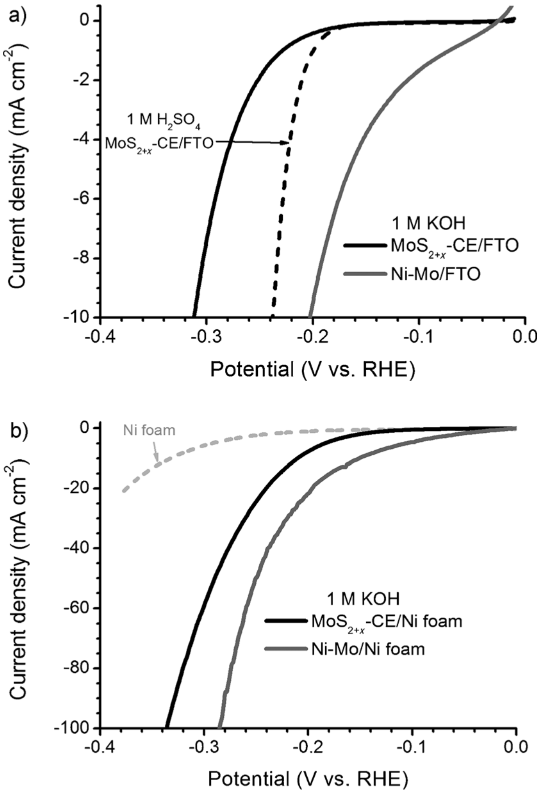

Figure 1. a) Linear sweep voltammetry (from positive to negative) of MoS_{2+x}–CE/FTO and Ni–Mo/FTO. b) Linear sweep voltammetry (from positive to negative) of MoS_{2+x}–CE/Ni foam and Ni–Mo/Ni foam. Conditions: 1 M KOH (pH 13.6), scan rate: 1 mV s^{-1}, iR drop corrected, the 5th linear sweep is shown.

Recently, Mo_2C,[20] MoB,[20] and Ni_2P[21,22] nanoparticles were reported as good HER catalysts in basic solutions. The activity of MoS_{2+x}–CE catalyst is similar to those catalysts, and higher than NiO_x and $Ni(OH)_2$ films (Table S1, SI). Ni–Mo is reported as one of the most active HER catalysts in alkaline solutions.[23] Figure 1 a shows the HER activity of Ni–Mo on FTO in 1 M KOH. The Ni–Mo/FTO electrode was prepared by passing a cathodic charge of 4.5 C cm^{-2}, corresponding to a catalyst loading of about 15 μg cm^{-2} (see SI).[24] The Ni–Mo catalyst is more active than MoS_{2+x} and requires an overpotential of 200 mV to reach 10 mA cm^{-2}. Both the MoS_{2+x} and Ni–Mo catalysts can be deposited on high surface area substrates such as Ni foam to give high current densities at modest overpotentials. Figure 1 b shows that MoS_{2+x} on Ni foam reaches 10 mA cm^{-2} at $\eta = 210$ mV, and 100 mA cm^{-2} at $\eta = 335$ mV overpotential. Ni–Mo on Ni foam reaches 10 mA cm^{-2} at $\eta = 150$ mV and 100 mA cm^{-2} at $\eta = 280$ mV overpotential. Figure S3 shows that the Faradaic yield for HER is close to 100 % for the MoS_{2+x}–CE catalyst.

Figure S4 shows the Tafel plot for the MoS_{2+x}–CE and Ni–Mo catalysts. For the MoS_{2+x}–CE catalyst, the Tafel slope is 84 mV dec^{-1} in 1 M KOH but 39 mV dec^{-1} in 1 M H_2SO_4. In comparison, the Ni–Mo catalyst has a Tafel slope of 119 mV dec^{-1} at modest overpotentials.

Because the MoS_{2+x} and Ni–Mo catalysts can be electrochemically deposited under mild conditions, they are attractive HER catalysts to integrate with a photocathode for PEC hydrogen production in alkaline solutions. The photocathode we chose is surface-protected p-type Cu_2O. Cu_2O is a promising low-cost material with a direct band gap of 2.0 eV. The material is suitable for capturing a large fraction of sunlight with a maximum theoretical solar-to-hydrogen (STH) efficiency of 18 % under AM 1.5 G solar illumination. Efficient PEC hydrogen production has been achieved on surface-protected Cu_2O using Pt, RuO_x, and MoS_{2+x} as HER catalysts, but only in acidic and near-neutral solutions.[25–27]

The protected p-Cu_2O photoelectrodes, Cu_2O/AZO/TiO_2, were prepared as previously described.[25,27] Following cathodic electrodeposition of Cu_2O, atomic layer deposition was used to apply a thin layer of aluminum-doped zinc oxide (AZO, 20 nm) to create a p–n junction with Cu_2O, and a layer of titanium oxide (TiO_2, 100 nm) was applied to protect the photovoltaic junction from the electrolyte solution. The MoS_{2+x} and Ni–Mo catalysts were deposited on the TiO_2 layer photoelectrochemically (Figure S5). Figure 2 shows scanning electron microscopy (SEM) images of the top and cross section of the catalyst-coated Cu_2O photocathodes. XPS analysis of the as-prepared photocathodes show that both catalysts were deposited conformally on the surface (Figure S6). The Mo/S ratio in the MoS_{2+x} is 1:1.7; the Ni/Mo ratio in Ni–Mo is 85:15, similar to values found in the literature.[9,24] The MoS_{2+x} film has a thickness of 30–50 nm, whereas the Ni–Mo film has a thickness of about 40 nm. Compared with Ni–Mo, the MoS_{2+x} film appeared rougher. Estimation of the catalyst loading from the total charge passed during photoelectrodeposition is complicated by the concomitant photoelectrochemical hydrogen evolution.

The catalyst-coated p-Cu_2O photocathodes were tested for hydrogen evolution under simulated AM 1.5 G (100 mW cm^{-2}) solar illumination in 1 M KOH. Figure 3 a displays the current–potential curves in the dark and under illumination. The onset potential of photocurrent ($j = -0.1$ mA cm^{-2}) is +0.48 V versus RHE for the MoS_{2+x}/

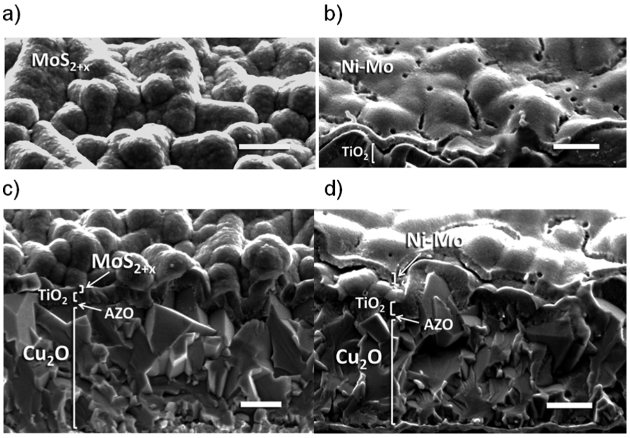

Figure 2. a) SEM image of the surface of a MoS_{2+x}/Cu_2O photoelectrode. b) SEM image of the surface of a Ni–Mo/Cu_2O photocathode. c) SEM image of the cross section of a MoS_{2+x}/Cu_2O photoelectrode. d) SEM image of the cross section of a Ni–Mo/Cu_2O photocathode. Scale bar: 200 nm.

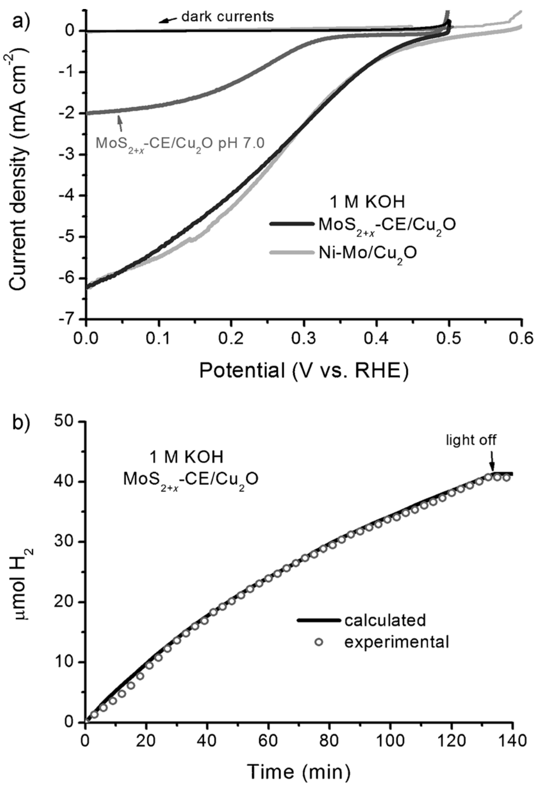

Figure 3. PEC performance of photocathodes in 1 M KOH. a) Current–potential curve for surface-protected photocathode activated for HER with MoS_{2+x} and Ni–Mo catalysts. MoS_{2+x}–CE/Cu_2O performance in pH 7.0 is also shown. b) Faradaic efficiency for a MoS_{2+x}–CE/Cu_2O photocathode biased at 0 V versus RHE. The volume of hydrogen produced during 130 min of illumination was measured using a gas-tight, home-made H cell calibrated for pressure and gas quantification.

Cu_2O photocathode, similar to the onset potential of an analogous photocathode at pH 1.0.[27] A photocurrent of $-6.3\ mA\,cm^{-2}$ was obtained at 0 V versus RHE, which is even higher than the photocurrent at pH 1.0 ($-5.7\ mA\,cm^{-2}$). Much lower photovoltage and photocurrents were obtained on the same photocathode at pH 7.0, indicating the influence of pH. Dark currents were negligible. The onset potential of photocurrent ($j = -0.1\ mA\,cm^{-2}$) is $+0.53$ V versus RHE for the Ni–Mo/Cu_2O photocathode. The more positive onset potential obtained with the Ni–Mo catalyst is consistent with its higher HER activity than MoS_{2+x}. Interestingly, the current densities at potentials negative of 0.45 V are nearly identical for the MoS_{2+x}/Cu_2O and Ni–Mo/Cu_2O photocathodes. Thus, at 0 V versus RHE, the Ni–Mo/Cu_2O photocathode also gives a current density of $-6.3\ mA\,cm^{-2}$. At this moment, it is unclear why the Ni–Mo catalyst gives a more positive onset potential but identical photocurrent densities at more negative potentials than the MoS_{2+x} catalyst. Electrochemical impedance spectroscopy will be applied to dissect the complex photoelectrochemical process. Figure 3 b shows that the MoS_{2+x}/Cu_2O photoelectrode has a quantitative Faradaic yield for hydrogen production.

The long term stability of the MoS_{2+x}/Cu_2O and Ni–Mo/Cu_2O photoelectrodes in 1 M KOH was evaluated under continuous AM 1.5 illumination at 0 V versus RHE. The photocurrents of both photoelectrodes decayed gradually over 10 h. The stability of these photoelectrodes is higher than an analogous MoS_{2+x}/Cu_2O photocathode at pH 1.0, of which the TiO_2 protective layer was dissolved and the photocathode lost completely its activity after 8 h (Figure S7). The deactivation of the devices in 1 M KOH is not due to the dissolution of the TiO_2 layer as in acidic solutions, but due to the formation of Ti^{3+} traps in TiO_2, evidenced by the darkening of the protective film after prolonged testing (Supporting Movie 2). Increasing the photovoltage generated by the buried p–n junction and improving the HER activity of the catalyst layer should enhance the extraction of photoexcited electrons for hydrogen production, thereby decreasing the trapping of electrons in the TiO_2 layer. This in turn should lead to higher stability.

In summary, we show for the first time that amorphous molybdenum sulfide is an active and stable hydrogen evolution catalyst in alkaline solutions. The molybdenum sulfide catalysts and a Ni–Mo catalyst are integrated onto surface-protected Cu_2O photocathodes. These catalyst-coated Cu_2O photoelectrodes exhibit high photoelectrochemical activity for hydrogen evolution in alkaline solutions. Photocurrents as high as $-6.3\ mA\,cm^{-2}$ have been obtained at 0 V versus RHE, which would correspond to 7.7 % STH efficiency in a tandem cell, in which the bias is provided by a second photoactive component. The photoelectrochemical hydrogen evolution has a quantitative Faradaic yield. Even though the Ni–Mo catalyst is a better electrocatalyst than MoS_{2+x} in alkaline solutions and gives a slightly more positive onset potential for hydrogen evolution for the p-Cu_2O photoelectrode, the photocurrent densities are identical at potentials more negative than 0.45 V versus RHE. The devices reported here are the first highly active photocathodes in alkaline solutions that make use of earth-abundant HER catalysts and inexpensive photoabsorbers. The development of these devices offers a new opportunity for efficient solar water splitting in basic medium.

Experimental Section

The conditions for the electrochemical and photoelectrochemical deposition of amorphous molybdenum sulfide films on conductive substrates and surface-protected Cu_2O have been previously reported by our group.[15,27] In brief, electrochemical deposition was done from a freshly prepared 2 mM ammonium tetrathiomolybdate solution [$(NH_4)_2MoS_4$, Aldrich, 99.97 %] in 0.1 M $NaClO_4$ (ABCR, 99 %). Different potentials were used to prepare the different electrodes. MoS_{2+x}–CE was deposited on TEC-15 fluorine-doped tin oxide (FTO; Nippon Sheet Glass) and Ni foam (95 % porosity, Goodfellow Cambridge Limited) substrates by constant potential electrolysis at −0.3 V versus RHE for 1 h. MoS_3–AE was deposited by constant potential electrolysis at 0.7 V versus RHE for 1 h. The photoelectrodeposition of MoS_{2+x}–CE on surface-protected Cu_2O was carried out under simulated AM 1.5 G solar illumination (1 sun) in a 0.2 mM $(NH_4)_2MoS_4$, 0.1 M $NaClO_4$ solution at a constant potential of 0.2 V versus RHE. The PEC deposition time was typically 50 min.

The nickel molybdenum (Ni–Mo) catalyst was deposited on FTO and Ni foam by electrochemical deposition. The nickel foam was pretreated by dipping for 1 min in 6 M HCl to increase the hydrophilicity of the substrate. The deposition was performed in a two-electrode setup with a nickel wire as counter electrode and the conductive substrate as working electrode. The procedure is similar to the one used by McKone et al.[24] The solution used for the deposition contained 325 $g L^{-1}$ $Ni(SO_3NH_2)$ (hydrate, crystalline, Alfa Aesar), 30 $g L^{-1}$ H_3BO_3 ($\geqq$99.5 %, Aldrich), and 5 $g L^{-1}$ $NaMoO_4$ (> 98 %, Aldrich). The pH was adjusted to 4.0 with H_2SO_4 (95–97 %, Merck). Electrodeposition was carried out at constant cathodic current density of −25 $mA cm^{-2}$ during 180 s. Photoelectrodeposition of Ni–Mo on surface-protected Cu_2O was done in a three-electrode-cell configuration with a Ni wire counter electrode and Ag/AgCl (KCl sat.) reference electrode. PEC deposition was carried out under simulated AM 1.5 illumination at constant potential of −0.2 V versus RHE for the Cu_2O photocathode. The deposition time was typically 180 s. Faradaic efficiency was measured using a cell calibrated for hydrogen volume measurement previously reported.[20,27]

Received: October 29, 2014

Keywords: cuprous oxide · hydrogen evolution · photocatalysis · photoelectrochemistry · water splitting

---

[1] M. Grätzel, *Nature* **2001**, *414*, 338 – 344.

[2] N. S. Lewis, D. G. Nocera, *Proc. Natl. Acad. Sci. USA* **2006**, *103*, 15729 – 15735.

[3] E. Fabbri, A. Habereder, K. Waltar, R. Kotz, T. J. Schmidt, *Catal. Sci. Technol.* **2014**, *4*, 3800 – 3821.

[4] L. Trotochaud, J. K. Ranney, K. N. Williams, S. W. Boettcher, *J. Am. Chem. Soc.* **2012**, *134*, 17253 – 17261.

[5] M. W. Louie, A. T. Bell, *J. Am. Chem. Soc.* **2013**, *135*, 12329 – 12337.

[6] R. D. L. Smith, M. S. Prévot, R. D. Fagan, S. Trudel, C. P. Berlinguette, *J. Am. Chem. Soc.* **2013**, *135*, 11580 – 11586.

[7] B. Seger, A. B. Laursen, P. C. K. Vesborg, T. Pedersen, O. Hansen, S. Dahl, I. Chorkendorff, *Angew. Chem. Int. Ed.* **2012**, *51*, 9128 – 9131; *Angew. Chem.* **2012**, *124*, 9262 – 9265.

[8] Y. Hou, B. L. Abrams, P. C. K. Vesborg, M. E. Björketun, K. Herbst, L. Bech, A. M. Setti, C. D. Damsgaard, T. Pedersen, O. Hansen, J. Rossmeisl, S. Dahl, J. K. Nørskov, I. Chorkendorff, *Nat. Mater.* **2011**, *10*, 434 – 438.

[9] E. L. Warren, J. R. McKone, H. A. Atwater, H. B. Gray, N. S. Lewis, *Energy Environ. Sci.* **2012**, *5*, 9653 – 9661.

[10] Q. Ding, F. Meng, C. R. English, M. Cabán-Acevedo, M. J. Shearer, D. Liang, A. S. Daniel, R. J. Hamers, S. Jin, *J. Am. Chem. Soc.* **2014**, *136*, 8504 – 8507.

[11] Y. Lin, C. Battaglia, M. Boccard, M. Hettick, Z. Yu, C. Ballif, J. W. Ager, A. Javey, *Nano Lett.* **2013**, *13*, 5615 – 5618.

[12] S. Ida, K. Yamada, T. Matsunaga, H. Hagiwara, Y. Matsumoto, T. Ishihara, *J. Am. Chem. Soc.* **2010**, *132*, 17343 – 17345.

[13] D. Merki, S. Fierro, H. Vrubel, X. Hu, *Chem. Sci.* **2011**, *2*, 1262 – 1267.

[14] C. G. Morales-Guio, X. Hu, *Acc. Chem. Res.* **2014**, *47*, 2671 – 2681.

[15] H. Vrubel, X. Hu, *ACS Catal.* **2013**, *3*, 2002 – 2011.

[16] D. Merki, X. Hu, *Energy Environ. Sci.* **2011**, *4*, 3878 – 3888.

[17] C. G. Morales-Guio, L.-A. Stern, X. Hu, *Chem. Soc. Rev.* **2014**, *43*, 6555 – 6569.

[18] A. B. Laursen, S. Kegnaes, S. Dahl, I. Chorkendorff, *Energy Environ. Sci.* **2012**, *5*, 5577 – 5591.

[19] J. Kibsgaard, Z. B. Chen, B. N. Reinecke, T. F. Jaramillo, *Nat. Mater.* **2012**, *11*, 963 – 969.

[20] H. Vrubel, X. Hu, *Angew. Chem. Int. Ed.* **2012**, *51*, 12703 – 12706; *Angew. Chem.* **2012**, *124*, 12875 – 12878.

[21] E. J. Popczun, J. R. McKone, C. G. Read, A. J. Biacchi, A. M. Wiltrout, N. S. Lewis, R. E. Schaak, *J. Am. Chem. Soc.* **2013**, *135*, 9267 – 9270.

[22] L. Feng, H. Vrubel, M. Bensimon, X. Hu, *Phys. Chem. Chem. Phys.* **2014**, *16*, 5917 – 5921.

[23] J. R. McKone, S. C. Marinescu, B. S. Brunschwig, J. R. Winkler, H. B. Gray, *Chem. Sci.* **2014**, *5*, 865 – 878.

[24] J. R. McKone, E. L. Warren, M. J. Bierman, S. W. Boettcher, B. S. Brunschwig, N. S. Lewis, H. B. Gray, *Energy Environ. Sci.* **2011**, *4*, 3573 – 3583.

[25] A. Paracchino, V. Laporte, K. Sivula, M. Grätzel, E. Thimsen, *Nat. Mater.* **2011**, *10*, 456 – 461.

[26] S. D. Tilley, M. Schreier, J. Azevedo, M. Stefik, M. Graetzel, *Adv. Funct. Mater.* **2014**, *24*, 303 – 311.

[27] C. G. Morales-Guio, S. D. Tilley, H. Vrubel, M. Grätzel, X. Hu, *Nat. Commun.* **2014**, *5*, 3059.